Application of NMRD to Hydration of Rubredoxin and a Variant Containing a $(Cys\text{-}S)_3Fe^{III}(OH)$ Site

Ivano Bertini,* Claudio Luchinat,† Kirill Nerinovski,* Giacomo Parigi,† Maddalena Cross,‡ Zhiguang Xiao,‡ and Anthony G. Wedd‡

*CERM and Department of Chemistry, University of Florence, Via Luigi Sacconi 6, 50019 Sesto Fiorentino, Italy; †CERM and Department of Agricultural Biotechnology, University of Florence, P. le delle Cascine 28, 50144 Florence, Italy; and ‡School of Chemistry, University of Melbourne, Parkville, Victoria, 3010, Australia

ABSTRACT Hydration of oxidized rubredoxin (Fe^{III}(S-Cys)$_4$ center) was investigated by ^{1}H and ^{17}O relaxation measurements of bulk water as a function of the applied magnetic field (nuclear magnetic relaxation dispersion). Oxidized rubredoxin showed an increased water ^{1}H relaxation profile with respect to the diamagnetic gallium derivative or reduced species. Analysis of the data shows evidence of exchangeable proton(s) ~4.0–4.5 Å from the metal ion, the exchange time being longer than 10^{-10} s and shorter than 10^{-5} s. The correlation time for the proton-electrons interaction is 7×10^{-11} s and is attributed to the effective electron relaxation time. Its magnitude is consistent with the large signal linewidths of the protein donor nuclei, observed in high resolution NMR spectra. For reduced rubredoxin, such correlation time is proposed to be smaller than 10^{-11} s. ^{17}O relaxation measurements suggest the presence of at least one long-lived protein-bound water molecule. Analogous relaxation measurements were performed on the C6S rubredoxin variant, whose iron(III) center has been previously shown to be coordinated to three cysteine residues and a hydroxide ion above pH 6. ^{1}H nuclear magnetic relaxation dispersion profiles indicate increased hydration with respect to the wild-type.

INTRODUCTION

There is a number of different ways in which water molecules interact with proteins, including population of specific cavities, access of solvent molecules to aspecific regions, and aspecific hydration (Wüthrich et al., 1992; Qian et al., 1993; Bai et al., 1995; Otting and Liepinsh, 1995; Venu et al., 1997; Otting, 1997; Bertini et al., 2000). The presence of water molecules surrounding a paramagnetic metal ion can be detected via magnetic interactions with the water protons. Chemical exchange between bulk and coordinated water frequently occurs at a rate higher than the relaxation rate of coordinated water protons, and this causes an increase in the proton relaxation rate of bulk water. Proton nuclear magnetic relaxation dispersion (^{1}H NMRD) is a technique based on the measurement of the longitudinal nuclear relaxation time of solvent water protons as a function of the magnetic field. The enhancement in relaxation with respect to the diamagnetic analog provides information on the dynamics of the paramagnetic metal ion-solvent interactions (such as proton exchange rates and correlation times for the proton-electrons interaction) as well as on the structure of the system (metal-proton distances, for example) (Koenig and Brown, 3d, 1990; Bayburt and Sharp, 1990; Gonzalez et al., 1994; Aime et al., 1994; Bertini et al., 1995b; Bertini et al., 1996; Kroes et al., 1996; Elst et al., 1997; Bligh et al., 1999; Caravan et al., 1999; Anelli et al., 2000; Hardcastle et al., 2000; Bertini et al., 2001a). Such measurements provide the sum of the contributions from water coordinated to the metal ion as long as it is in fast exchange, exchangeable protons anchored at a protein site, and outer-sphere water molecules (Hwang and Freed, 1975; Koenig et al., 1981; Zewert et al., 1994; Chen et al., 1998; Aime et al., 2000; Botta, 2000; Bertini et al., 2001b).

Whereas ^{1}H and ^{2}H relaxation are affected by hydrogen exchange between water and protein, ^{17}O NMRD does not suffer from this complication and it has been established that the amplitude of the dispersion, whose inflection corresponds to the protein rotational correlation time τ_R, yields direct information on long-lived water molecules, i.e., water molecules that are bound to the protein with exchange times longer than τ_R (Denisov and Halle, 1995a; Denisov and Halle, 1996). It was shown that a small number of water molecules trapped in cavities or coordinated to protein-bound metal ions was responsible of the ^{17}O NMRD dispersion observed for the small proteins bovine pancreatic trypsin inhibitor, ubiquitin and calbindin D_{9k} (Denisov and Halle, 1995a; Denisov and Halle, 1995b; Denisov and Halle, 1995c). Furthermore, it has been demonstrated that a single water molecule is immobilized in the oxidized forms of cyt *c* and cyt b_5 but is released upon reduction (Bertini et al., 2001c). The residence times of such water molecules, although longer than τ_R, are usually shorter than the reciprocal of the frequency separation between the signals of free and bound water, so that such water molecules are not observable directly by high-resolution NMR spectroscopy.

The present work aimed at the investigation of hydration of a simple protein as the oxidized rubredoxin (Rd), in which iron(III) is coordinated by four cysteines. The protein and its redox properties have been extensively studied (Cammack, 1992; Ayhan et al., 1996; Beinert et al., 1997; Meyer et al.,

Submitted June 3, 2002, and accepted for publication September 9, 2002.

Address reprint requests to Ivano Bertini, Fax: +39-055-4574271; E-mail: bertini@cerm.unifi.it.

0006-3495/03/01/545/07 $2.00

1997; Xiao et al., 1998; Eidsness et al., 1999; Xiao et al., 2001; Bonomi et al., 2002). The approach is that of measuring ^{1}H NRMD profiles. Such measurements provide information on the presence of exchangeable protons close to the paramagnetic center. ^{17}O NMRD profiles were also acquired to investigate whether such protons belong to long-lived water molecules. The presence of water molecules near the redox site could affect the reduction potential by enhancing the affinity of the site for an electron. The interpretation of the data profits from analogous measurements on the variant C6S, in which the coordination is provided by three cysteines and a solvent hydroxide. The present data reveal both the presence of ordered water in the proteins and of fast exchangeable proton(s) close to the Fe(III) site, which are not clearly revealed in the x-ray data of wild-type Rd (Day et al., 1992; Sieker et al., 1994; Dauter et al., 1996).

METHODS

Proteins

Isolation of Fe(III) forms of wild-type and C6S proteins has been described previously (Ayhan et al., 1996; Xiao et al., 1998; Xiao et al., 2001). For substitution with Ga(III), expressed wild-type or C6S protein was precipitated by addition of trichloracetic acid and β-mercaptoethanol to concentrations of ~5–10% and 0.15 M, respectively, producing a white precipitate under a yellow supernatant. After centrifugation (7,600 rpm, 5 min), the protein pellet was washed with trichloracetic acid solution (5%) containing β-mercaptoethanol (50 mM), centrifuged (7,600 rpm, 5 min), and redissolved in a minimum volume of Tris base (0.5 M) containing β-mercaptoethanol (0.15 M). After a twofold dilution with water, the precipitation and dissolution procedure was repeated. The final pH was ~8. A twofold molar excess of gallium(III) nitrate (200 mM) was added. After incubation on ice (1 h), a precipitate was removed by filtration. The solution was diluted fourfold with buffer (Tris-HCl, 50 mM, pH 7.8) before application to an anion exchange column (1.5 cm × 5.0 cm), which had been equilibrated with Tris (50 mM, pH 7.8). A salt gradient (0.1–0.3 M) was applied and a single symmetrical peak eluted. The protein peak was collected, concentrated (Centricon), and loaded onto a high-resolution UNO Q column (3 cm × 0.5 cm, Bio-Rad) equilibrated with buffer (Tris-HCl, 50 mM, pH 7.8). A salt gradient (0.1–0.3 M) was applied using the automated Biologic System (Bio-Rad). A single symmetrical peak eluted at the salt concentration expected for the Fe(III) forms of Rd. Peaks assignable to apoprotein (Cross et al., 2002) were absent. The UV-visible electronic spectrum consisted of a single peak at 280 nm with no absorption above background in the visible region, consistent with the removal of Fe(III) and the incorporation of Ga(III). The Ga(III) forms of both wild-type and C6S proteins exhibited well-resolved ^{1}H-^{15}N HSQC NMR spectra with the expected number of crosspeaks.

^{1}H NMRD

Longitudinal water proton relaxation rates were measured with a Koenig-Brown field cycling relaxometer (0.02–50 MHz proton Larmor frequency range) (Bertini et al., 2001a). The instrument provides R_1 values with an error of ~1%. NMRD profiles were obtained by plotting proton relaxation rates as a function of applied magnetic field.

Using known molar absorptivities at 280 nm (Xiao et al., 1998), the concentrations of oxidized Fe(III) Rd in wild-type and C6S forms in phosphate buffer (20 mM; pH 7.0) were determined to be 6.86 and 6.72 mM, respectively. The concentrations of the respective Ga(III)-substituted Rd, used to evaluate the diamagnetic contribution, were 6.52 and 3.03 mM, assuming the molar absorptivities at 280 nm to be those of the Zn(II) derivatives.

^{17}O NMRD

Water ^{17}O NMR measurements on 20% ^{17}O-enriched water samples were performed between 4.0 and 81.4 MHz (corresponding to 29.5 and 600 MHz for protons) with commercially available spectrometers (Bruker AVANCE 600, Bruker DRX 500, Bruker AVANCE 400, Bruker MSL 200) and with a Bruker CXP 90 electromagnet with variable field capability. The sample temperature was maintained at 300.0 ± 0.1K by a thermostated air flow. Longitudinal relaxation times were measured by the inversion recovery pulse sequence (180°-τ-90°). Phase cycling was used to eliminate residual pulse length and phase errors. At low fields, up to 256 transients were accumulated for each τ value to improve signal-to-noise ratio. Each relaxation experiment comprised 17 τ values in the interval (0.05–5.0)T_1. The relaxation times were evaluated from exponential nonlinear fits to the 17 data points using standard software. Measurement of the bulk water relaxation rate, R_{bulk} = 134.1 ± 0.7 s^{-1}, was carried out before each experiment and served as a temperature check on the different spectrometers.

Sample concentrations of Fe(III) Rd in wild-type and C6S variant forms were, respectively, 3.72 and 3.47 mM in CAPS buffer (20 mM, pH 9.0).

RESULTS

^{1}H NMRD

Profiles were acquired for both Fe(III) and Ga(III) forms of the wild-type and C6S Rds at 283 and 298 K. The Ga(III) samples provided the diamagnetic contribution to relaxation, as the experimental values obtained for the Fe(III) samples are the sum of the diamagnetic and paramagnetic contributions:

$$R_1 = R_{1dia} + R_{1para}. \quad (1)$$

Experimental R_1 data, corrected for the diamagnetic contribution and normalized at 1 mM protein solution, are reported in Fig. 1. They can be analyzed in terms of binding and outer-sphere effects, according to existing theories (Bertini et al., 1995a, 2001a).

R_{1para} can arise from bound and/or outer-sphere fast diffusing water protons, as well as fast exchanging protein protons, experiencing dipolar interaction with the unpaired electrons localized on the metal site (Bertini et al., 2001a):

$$R_{1para} = f_m \sum_i (T_{1Mi} + \tau_{Mi})^{-1} + R_{os} \quad (2)$$

where f_m is the mole fraction of the paramagnetic metal, T_{1Mi} are the relaxation times of each proton due to the paramagnetic center, and τ_{Mi} are their exchange times. The first term in Eq. 2 is due to both water or exchangeable protein protons at fixed distances r_i from the paramagnetic center; the latter, R_{os}, is due to water protons diffusing freely close to the paramagnetic center. The values of T_{1Mi} depend on r_i^{-6} and that of R_{os} on the distance of closest approach, d, of diffusing water protons. Actually, R_{os} depends also on the

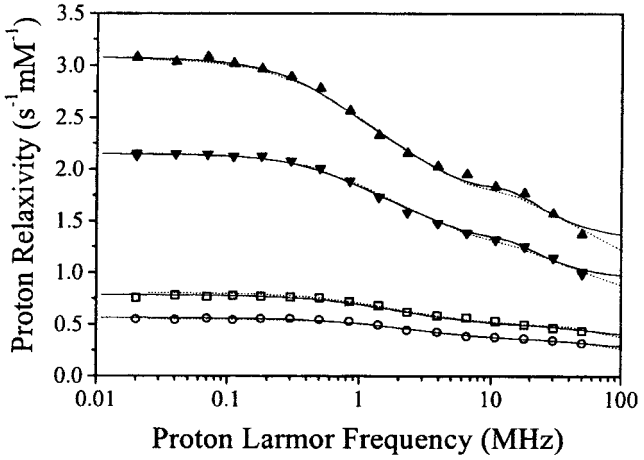

FIGURE 1 Paramagnetic enhancements to ^{1}H NMRD profiles of wild-type (*open symbols*) and C6S (*filled symbols*) Rd at 298 K (○ and ▼, respectively) and 283 K (□ and ▲, respectively). Solid lines and dotted lines represent the best fit curves calculated on the assumption of a rhombic component of ZFS $E/D = 0$ and $E/D = 1/3$, respectively. All other parameters are reported in Table 1.

diffusional correlation time $\tau_D = d^2/D_{diff}$, where D_{diff} is the diffusion coefficient, according to the following equation:

$$R_{os} = \frac{32}{405}\pi\left(\frac{\mu_0}{4\pi}\right)^2 \frac{1000[\mathrm{Rd}]N_A\gamma_I^2 g_e^2\mu_B^2 S(S+1)}{dD_{diff}} \times \{7J(\omega_S) + 3J(\omega_I)\} \quad (3)$$

where $J(\omega) = (1 + 5z/8 + z^2/8)/(1 + z + z^2/2 + z^3/6 + 4z^4/81 + z^5/81 + z^6/648)$ and $z = [2(\omega\tau_D + (\tau_D/\tau_S))]^{-1/2}$.

All terms in Eq. 2 depend on temperature: T_{1M}^{-1} may either decrease or increase with increasing temperature, depending on the correlation time τ_c that modulates the relaxation process; τ_M^{-1} always increases with increasing temperature; R_{os} usually decreases with increasing temperature, because of its dependence on the diffusion coefficient, although its exact temperature dependence may not be obvious due to the τ_D/τ_s term. However, the larger changes are due to τ_M, which decreases significantly with increasing temperature, thus determining a large increase in R_{1para}. The temperature dependence of the paramagnetic contribution to the NMRD profiles of both wild-type and C6S Rd shows that R_{1para} decreases with increasing temperature. This indicates that τ_M is not dominating with respect to T_{1M} and can thus be neglected in Eq. 2. Therefore, the NMRD data are sensitive to solvent accessibility to the metal site through either anchored or outer-sphere contributions or both. The difference between bound and outer-sphere water molecules is due to the residence time. The water is referred to as bound if its residence time is longer than the diffusional correlation time.

A quantitative analysis of the paramagnetic enhancement of ^{1}H NMRD profiles was performed using a program described in (Bertini et al., 1995a). A good fit for the data relative to the wild-type protein could be obtained only if comparable contributions from both anchored waters and outer-sphere effects were imposed. As expected (Bertini et al., 1995b), good agreement could only be obtained by inclusion of a modest zero field splitting (ZFS) parameter, D, of the $S = 5/2$ multiplet of the Fe(III) ion. Two extreme cases were considered, one with axial ZFS (*solid lines* in Fig. 1) and another with maximal rhombicity ($E/D = 1/3$) (*dotted lines* in Fig. 1). In fact, Rd is reported in most cases to have a rhombic ZFS, with rhombicity $E/D \approx 1/3$ (Guigliarelli and Bertrand, 1999). The best fit parameters are shown in Table 1. At low fields, they indicate contributions from inner-sphere molecules of 0.30 s^{-1} mM^{-1} and from outer-sphere molecules of 0.26 s^{-1} mM^{-1}. The fits provide estimates in the range 7–10 $\times$ 10^{-11} s for the correlation time for nuclear relaxation (τ_c). τ_c is the smallest of the rotational, exchange, and electron relaxation times. As estimated from the molecular weight of the protein, the rotational time τ_R is expected to be $\sim 2 \times 10^{-9}$ s (see later). The water proton exchange time is also expected to be longer than 10^{-10} s. Therefore, the correlation time coincides with the electron relaxation time τ_s. The τ_s values obtained from the fits are reasonable for high spin Fe(III) (Bertini et al., 2001a) and consistent with estimates (Bertini et al., 1999) from high resolution NMR data (Xia et al., 1995).

The metal-proton distance parameters (r and d for inner-sphere and outer-sphere contributions, respectively) obtained for wild-type Rd are also reasonable for the topology of the protein-solvent interface in the neighborhood of the metal center. The data may be indicative of a water molecule (i.e., two protons) hydrogen bonded to some hydrophilic residues in the cavity at an average distance of 4.5–4.3 Å or, alternatively, with a single exchangeable protein proton at 4.0–3.8 Å from the metal. An r value >4 Å is consistent with the absence of metal-coordinated water. On the other hand, the relatively large d value (9–10 Å) is not surprising as the outer-sphere theory holds for a spherical particle where d is the distance of closest approach from any direction, whereas in this case the approach is restricted within a solid angle which is much smaller than spherical. In case the fit is performed by dividing by two the value of R_{os} as calculated by Eq. 3 to consider the fact that water molecules may diffuse until a distance d only, for instance, in a semisphere, d decreases to 7.0–8.0 Å, and r increases to 4.6–4.4 Å, i.e., of 0.1 Å only. This makes us confident of the reliability of the results of the present fit.

In the case of reduced Rd, the ^{1}H NMRD profile was the same as that of the diamagnetic Ga(III) derivative within the experimental error. The lack of paramagnetic relaxation enhancement is likely to be due to a sizably shorter electron relaxation time, τ_s, whose upper limit can be estimated $\sim 10^{-11}$ s. High resolution ^{2}H NMR data (Xia et al., 1995) are consistent with a sizably shorter τ_s for reduced Rd.

The NMRD profiles for the C6S variant are dramatically higher than for the wild-type. Accordingly, the same type of data analysis (see Table 1) provides metal-proton distance parameters that are sensibly smaller than those estimated for

TABLE 1 Best fit parameters for the ^{1}H NMRD profiles (Fig. 1) of Rd proteins in the cases *E/D* = 0 and *E/D* = 1/3

	Wild-type				C6S			
	E/D = 0		*E/D* = 1/3		*E/D* = 0		*E/D* = 1/3	
Temperature, K	283	298	283	298	283	298	283	298
τ_s (10^{-12} s)	98 ± 9	72 ± 16	98 ± 19	70 ± 8	203 ± 16	144 ± 21	230 ± 23	160 ± 16
r (Å)*	4.54 ± 0.13		4.26 ± 0.14		3.83 ± 0.17		3.98 ± 0.08	
	(4.04 ± 0.12)		(3.80 ± 0.13)		(3.41 ± 0.15)		(3.54 ± 0.07)	
D (cm^{-1})	≥1.5†		≥1.5†		0.25 ± 0.03‡		0.80 ± 0.08‡	
d (Å)	9.0 ± 0.5§		10.5 ± 0.6		6.5 ± 0.3§		7.6 ± 0.3	

Errors are calculated with a Monte Carlo procedure.
The diffusion coefficients D_{diff} were fixed to 1.3 × 10^{-5} cm^2/s and 2 × 10^{-5} cm^2/s at 283 and 298 K, respectively. The rotational time τ_R was fixed to 2 × 10^{-9} s.
*Assuming 2 (or 1) equidistant protons.
†The angle θ between the metal-proton(s) direction and the z axis of the molecular frame was 0° for wild-type and 55° for C6S Rd.
‡The angle θ between the metal-proton(s) direction and the z axis of the molecular frame was 0° for both Rd proteins.
§It results τ_D = 620 × 10^{-12} s and 410 × 10^{-12} s at 283 and 298 K, respectively, for the wild-type, and τ_D = 330 × 10^{-12} s and 210 × 10^{-12} s at 283 and 298 K, respectively, for the C6S variant.

the wild-type protein. In fact, at low fields, the inner-sphere contribution to relaxivity is 1.2 s^{-1} mM^{-1} and the outer-sphere contribution to relaxivity is 1.0 s^{-1} mM^{-1}. We have no information on the rhombicity of ZFS in the mutant, so that the values of the fitting parameters should be considered in the range provided by the two limit conditions of $E/D = 0$ and $E/D = 1/3$. As a result, the distance of the closest water molecule decreases from 4.5–4.3 Å to 3.8–4.0 Å; d decreases from 9-10 to 6.5–7.6 Å. In case the fit is performed by considering that water molecules may diffuse in a semisphere only, d becomes 4.4–5.5 Å, and r 3.9–4.1 Å. Again, the value of r is changed of 0.1 Å only. This indicates that the sizable difference in r values between wild-type and mutant Rd is unchanged if water molecules freely diffuse only in a semisphere. In any case, no first-sphere exchangeable protons are visible by NMR, thus ruling out fast exchange of the coordinated hydroxide proton. Still, bound exchangeable protons are closer to the metal ion than in the wild-type case. It is also interesting to note that substitution of S with O also leads to an increase in the electron relaxation time by about a factor 2.

^{17}O NMRD

Fig. 2 shows the NMRD profiles of water ^{17}O T_1^{-1} as a function of the ^{17}O Larmor frequency at 300 K for both wild-type and C6S mutant Rd. The bulk water relaxation has been subtracted, and the data normalized to a water:protein molar ratio of 1. Measurements at lower temperature (not shown) indicate that the relaxation values are not limited by exchange. Calculations based on the data obtained from the analysis of the ^{1}H NMRD show that paramagnetism contributes negligibly to ^{17}O relaxation. Under these conditions, the longitudinal quadrupolar relaxation rate enhancement of ^{17}O due to the interaction with the protein, $R_1 - R_{bulk}$, is the dominant contribution and, in turn, is given by the sum of two terms (Eq. 4):

$$R_1 - R_{bulk} = \alpha + \beta\tau_C\left(\frac{0.2}{1+\omega_I^2\tau_C^2} + \frac{0.8}{1+4\omega_I^2\tau_C^2}\right) \quad (4)$$
$$\alpha = (N_S/N_T)(\langle R_S\rangle - R_{bulk})$$
$$\beta = \left(N_I^*/N_T\right)(\omega_Q S_I)^2$$

where ω_I is the ^{17}O Larmor frequency in rad s^{-1} and N_S, N_I^*, and N_T are the number of surface water molecules, the effective number of long-lived water molecules, and the total number of water molecules per protein molecule in the solution, respectively. $\langle R_S\rangle$ is the average intrinsic spin relaxation rate of surface water, $\omega_Q = 7.61 \times 10^6$ rad s^{-1} is the rigid-lattice nuclear quadrupole frequency (Halle et al., 1999), and S_I is the average (rms) orientational order parameter for the ^{17}O nuclei of long-lived water molecules.

The parameter α represents the relaxation rate enhancement above the bulk value R_{bulk}. It gives the value of the

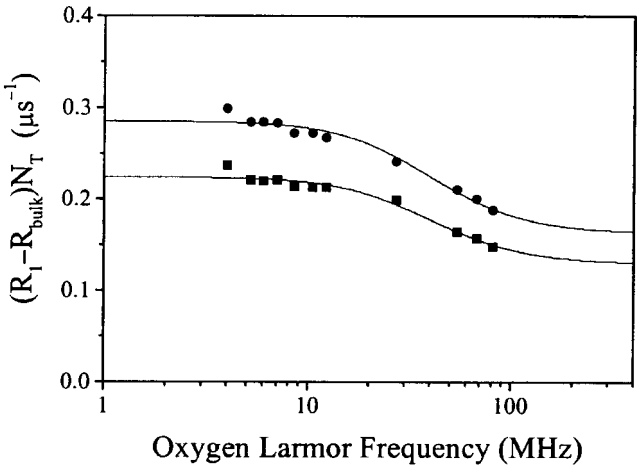

FIGURE 2 ^{17}O NMRD profiles (expressed as relaxation enhancements × the total number of water molecules per protein molecule, N_T) of solutions containing the wild-type (*squares*) and C6S variant (*circles*) forms of Fe(III) Rd. T = 300 K. Lines represent the best fit curves.

high-field plateau and is a consequence of the large number, N_S, of water molecules at the protein surface with residence times much shorter than the rotational correlation time, τ_R, of the protein. It may also contain contributions due to local motions of internal water molecules. The value $\beta\tau_C$ describes the dispersion step with inflection point determined by the effective correlation time τ_C given by $\tau_C^{-1} = \tau_R^{-1} + \tau_M^{-1}$ where τ_M is the lifetime of the water molecule in the bound state.

The experimental dispersion curves have been fitted to Eq. 4, and the results are shown in Table 2 and in Fig. 2. The fits were performed under the assumption of a single τ_C value, which was found to be $\tau_C \approx 2.3 \times 10^{-9}$ s, i.e., a value consistent with the Stokes-Einstein estimate of τ_R for a protein of the size of Rd.

The quantity $N_I^* S_I^2$, obtained from the low-field dispersions and the τ_C values, represents the minimal number of long-lived waters, assuming they are orientationally ordered ($S_I^2 = 1$). If the long-lived waters experience some librational motions ($S_I^2 < 1$) and/or their lifetime is of the order or longer than their intrinsic ^{17}O relaxation time, their number can be larger than the above quantity. Best fit data show that at least one water molecule is indeed associated with the protein (Table 2). In the mutant form $N_I^* S_I^2$ increases from 0.74 ± 0.21 to 0.94 ± 0.21, i.e., it remains below 1. Although almost within the error, the increase may indicate that this water is more rigid than for wild-type, or that there is a larger fractional occupation of a second water site. The residence time of a water molecule of this type must be in the range $2 \times 10^{-9} - 8 \times 10^{-6}$ s, i.e., longer than the rotational time of the protein and shorter than their intrinsic relaxation time (Denisov and Halle, 1996; Halle et al., 1999). Even if the x-ray structures (PDB numbers: 5RXN, 1FHH, 1IRO) of wild-type Rd do not clearly display any buried water, there is evidence that some water molecules are in deep surface pockets (like W2 and W4 in 1IRO), and could thus be responsible of the observed dispersion. All these waters are anyway far from the paramagnetic center (more than 8 Å) and cannot thus be responsible of the observed proton relaxation. Furthermore, it is reasonable to assume that the position and properties of such molecules is not affected much by the C6S mutation.

As proposed by Halle et al. (Halle et al., 1999), the physical meaning of the high-field plateau is expressed by the quantity N_S ($\langle R_S\rangle/R_{bulk} - 1$), where N_S is the number of waters significantly different from bulk and $\langle R_S\rangle$ is their average relaxation rate. The value of N_S can be interpreted as the number of water molecules in the monolayer around the protein molecule (Halle et al., 1999). The dynamic retardation factor $\langle R_S\rangle/R_{bulk}$ lies in the range of 5–7 for most investigated native globular proteins (Denisov and Halle, 1996) and any deviation from that value, in principle, can indicate the existence of few water molecules in the protein environment with a residence time longer than tens of picoseconds but shorter or equal to τ_R. There is a modest difference in the high field plateau, and thus in N_S ($\langle R_S\rangle/R_{bulk} - 1$) values, between wild-type and mutant, which is barely significant in the light of the uncertainties obtained from the fit (Table 2). If so, it might be due to a slight change in the water network near to the metal binding site. Indeed, as shown by ^1H NMRD, the mutation makes the metal binding site more open to water, and few water molecules could approach the metal ion with exchange time shorter than, or of the same order of, the rotational time of the protein.

TABLE 2 Best fit parameters for ^{17}O NMRD profiles (Fig. 2) for Rd proteins

	Wild-type	C6S
N_S ($\langle R_S\rangle/R_{bulk} - 1$) 10^3	1.0 ± 0.1	1.2 ± 0.1
$\langle R_S\rangle/R_{bulk}$	6.4 ± 0.3	7.8 ± 0.4
$N_I^* S_I^{2\dagger}$	0.74 ± 0.21	0.94 ± 0.21
τ_C (10^{-9} s)	2.3 ± 0.5	

Errors are calculated with a Monte Carlo procedure.
†The difference in $N_I^* S_I^2$ between the wild-type and the C6S variant is $\Delta(N_I^* S_I^2) = 0.20 \pm 0.10$.

DISCUSSION

Water proton relaxation measurements of solutions of oxidized Rd provide significant information on the hydration of the protein, even if water is not directly coordinated to the paramagnetic center. Exchangeable protons at around 4.4 Å from the metal ion are detected, with a residence time larger than τ_s (10^{-10} s). The presence of such exchangeable protons is not clearly expected by looking at the crystal structure of the protein. Although in the crystal structure no water is found close to the iron ion, it is possible that in solution, water molecule(s) can approach the paramagnetic site. Analysis of the x-ray structure of oxidized and reduced wild-type Rd suggested that transient penetration of water molecules can occur in reduced wild-type Rd due to conformational changes of leucine 41 (Min et al., 2001); it is possible that to some extent conformational changes of leucine 41 may occur in solution also for the oxidized protein, although they are not observed in the crystal form.

^{17}O relaxation measurements indicate the presence of at least one long-lived water molecule. Because ^{17}O relaxation is independent on the distance of water molecules to the metal ion, two possibilities should be discussed, according to the hypothesis that such water molecule(s) is close or far from the metal binding site. If the water is close to the metal, both ^1H and ^{17}O relaxation are likely to be related to the same water molecule, probably anchored to the protein through H-bonds. However, protein crystal structures indicate the presence of at least two water molecules in deep surface pockets far from the paramagnetic center, which may be responsible for the inflection in the ^{17}O profile. In this case, ^1H and ^{17}O obviously sample different phenomena, and there is not evidence whether the fast exchanging protons detected by ^1H measurements are

protein protons or water protons. Inspection of residues close to the metal ion indicates the absence of suitable candidates for fast exchangeable protein protons. Therefore, the increase in proton relaxivity observed for the mutant is more likely to be due to the presence of additional water protons.

The increased hydration in the C6S mutant is consistent with a somewhat higher solvent accessibility of the metal site brought about by a more open conformation imposed by the serine 6 that allows a hydroxide ion to enter the metal first coordination sphere. Such increased solvent accessibility may also contribute, at least in part, to the slight increase in $N_I^* S_I^2$ and N_S ($\langle R_S \rangle / R_{bulk} - 1$) from the wild-type to the C6S mutant, obtained from ^{17}O data, as it would be the case if the water molecules that can get close to the metal in the mutant have residence times longer than τ_s (to account for the ^1H NMRD data) but shorter than, or of the order of, τ_R.

The peculiar behavior of the C6S variant contrasts with the other C-to-S variants, C9S, C39S, and C42S, where a serinate oxygen coordinates the metal ion with minimum alteration of the native structure. The increased hydration of the C6S variant with respect to the wild-type (and most likely also with respect to the other C-to-S variants) could be a further determinant of the anomalous reduction potential of the C6S variant. At high pH, the reduction potential of wild-type Rd is −85 mV, whereas it is −125 mV for C6S and around −200 mV for the other three C-to-S variants (Xiao et al., 1998; Xiao et al., 2001). In all cases, the charge of the metal site passes from −1 to −2 upon reduction. Although it is possible that $H\text{-}O^-$ versus $R\text{-}O^-$ coordination may by itself account for the striking difference between the C6S variant and the other three C-to-S variants, increased solvent accessibility is expected to favor the more highly charged reduced state $[Fe^{II}S_3O]^{2-}$. This would lower the reduction enthalpy, and increase the reduction potential with respect to the other three C-to-S variants.

This work was supported by a grant from the Australian Research Council (A10020211 to A.G.W); by MIUR ex 40%, Italy; the European Union (contracts HPRI-CT-1999-00009, HPRI-CT-2001-50028, and BIO4-CT98-0156); CNR, Progetto Finalizzato Biotecnologie, Italy (contract 990039349); and CNR, Comitato Nazionale per le Scienze Chimiche, Italy (contract 970113349).

REFERENCES

Aime, S., M. Botta, M. Fasano, S. Paoletti, P. L. Anelli, F. Uggeri, and M. Virtuani. 1994. NMR evidence of a long exchange lifetime for coordinated water in Ln(III)-bis(methyl amide)-DTPA complexes (Ln = Gd, Dy). *Inorg. Chem.* 33:4707–4711.

Aime, S., M. Botta, L. Frullano, S. Geninatti Crich, G. Giovenzana, R. Pagliarin, G. Palmisano, F. Riccardi Sirtori, and M. Sisti. 2000. [GdPCP2A(H2O)2]$^-$: A paramagnetic contrast agent designed for improved applications in magnetic resonance imaging. *J. Med. Chem.* 43:4017–4024.

Anelli, P. L., I. Bertini, M. Fragai, L. Lattuada, C. Luchinat, and G. Parigi. 2000. Sulfonamide-functionalised gadolinium DTPA complexes as possible contrast agents for MRI: a relaxometric investigation. *Eur. J. Inorg. Chem.* 3:625–630.

Ayhan, M., Z. Xiao, M. J. Lavery, A. M. Hamer, K. W. Nugent, S. D. B. Scrofani, J. M. Guss, and A. G. Wedd. 1996. The rubredoxin from clostridium pasteurianum: mutation of the conserved glycine residues 10 and 43 to alanine and valine. *Inorg. Chem.* 35:5902–5911.

Bai, Y. W., T. R. Sosnick, L. Mayne, and S. W. Englander. 1995. Protein folding intermediates: native-state hydrogen exchange. *Science.* 269:192–197.

Bayburt, T., and R. R. Sharp. 1990. Electron and nuclear-spin relaxation in an integer spin system, tris-(acetylacetonato)Mn(III) in solution. *J. Chem. Phys.* 92:5892–5899.

Beinert, H., R. H. Holm, and E. Münck. 1997. Iron-sulfur clusters: nature's modular multipurpose structures. *Science.* 277:653–659.

Bertini, I., M. Fragai, C. Luchinat, and G. Parigi. 2001b. Solvent 1H NMRD study of hexaaquochronium(III): inferences on hydration and electron relaxation. *Inorg. Chem.* 40:4030–4035.

Bertini, I., O. Galas, C. Luchinat, L. Messori, and G. Parigi. 1995b. A theoretical analysis of the ^1H nuclear magnetic relaxation dispersion profiles of diferric transferrin. *J. Phys. Chem.* 99:14217–14222.

Bertini, I., O. Galas, C. Luchinat, and G. Parigi. 1995a. A computer program for the calculation of paramagnetic enhancements of nuclear relaxation rates in slowly rotating systems. *J. Magn. Reson. Ser. A.* 113:151–158.

Bertini, I., P. Hajieva, C. Luchinat, and K. Nerinovski. 2001c. Redox-dependent hydration of cytochrome c and cytochrome b(5) studied through ^{17}O NMRD. *J. Am. Chem. Soc.* 123:12925–12926.

Bertini, I., J. G. Huber, C. Luchinat, and M. Piccioli. 2000. Protein hydration and location of water molecules in oxidized horse heart cytochrome c by (1)H NMR. *J. Magn. Reson.* 147:1–8.

Bertini, I., C. Luchinat, G. Mincione, G. Parigi, G. T. Gassner, and D. P. Ballou. 1996. NMR studies on *Phtalate dioxygenase*: evidence for displacement of water on binding substrate. *J. Biol. Inorg. Chem.* 1:468–475.

Bertini, I., C. Luchinat, and G. Parigi. 2001a. Solution NMR of Paramagnetic Molecules. Elsevier, Amsterdam.

Bertini, I., C. Luchinat, and A. Rosato. 1999. NMR spectra of iron-sulfur proteins. *In* Adv. Inorg. Chem. A. G. Sykes and, R., Cammack, editors. Academic Press, San Diego. 251–282.

Bligh, S. W., A. H. Chowdhury, D. Kennedy, C. Luchinat, and G. Parigi. 1999. Non-ionic bulky Gd(III) DTPA-bisamide complexes as potential contrast agents for magnetic resonance imaging. *Magn. Res. Med.* 41:767–773.

Bonomi, F., A. E. Burden, M. K. Eidsness, D. Fessas, S. Iametti, D. M. Kurtz, Jr., S. Mazzini, R. A. Scott, and Q. Zeng. 2002. Thermal stability of the [Fe(SCys)(4)] site in Clostridium pasteurianum rubredoxin: contributions of the local environment and Cys ligand protonation. *J. Biol. Inorg. Chem.* 7:427–436.

Botta, M. 2000. Second coordination sphere water molecules and relaxivity of gadolinium(III) complexes: implications for MRI contrast agents. *Eur. J. Inorg. Chem.* 3:399–576.

Cammack, R. 1992. Iron-sulfur clusters in enzymes: themes and variations. *Adv. Inorg. Chem.* 38:281–322.

Caravan, P., J. J. Ellison, T. J. McMurry, and R. B. Lauffer. 1999. Gadolinium(III) chelates as MRI contrast agents: structure, dynamics, and applications. *Chem. Rev.* 99:2293–2351.

Chen, J. W., R. L. Belford, and R. B. Clarkson. 1998. Second-sphere and outer-sphere proton relaxation of paramagnetic complexes: from EPR to NMRD. *J. Phys. Chem.* 102:2117–2130.

Cross, M., Z. Xiao, E. M. Maes, R. S. Czernuszawicz, S. C. Drew, J. R. Pilbrow, G. N. George, and A. G. Wedd. 2002. Removal of a cysteine ligand from rubredoxin: assembly of Fe_2S_2 and $Fe(S\text{-}Cys)_3$ (OH) centres. *J. Biol. Inorg. Chem.* 7:781–790.

Dauter, Z., K. S. Wilson, L. C. Sieker, J. M. Moulis, and J. Meyer. 1996. Zinc- and iron-rubredoxins from C *lostridium pasteurianum* at atomic resolution: a high-precision model of a ZnS4 coordination unit in a protein. *Proc. Natl. Acad. Sci. USA.* 93:8836–8840.

Day, M. W., B. T. Hsu, L. Joshua-Tor, Z. H. Zhou, M. W. Adams, and D. C. Rees. 1992. X-ray crystal structures of the oxidized and reduced forms of the rubredoxin from the marine hyperthermophilic archaebacterium *Pyrococcus furiosus*. *Protein Sci.* 1:1494–1507.

Denisov, V. P., and B. Halle. 1995a. Protein hydration dynamics in aqueous solution: a comparison of bovine pancreatic trypsin inhibitor and ubiquitin by oxygen-17 spin relaxation dispersion. *J. Mol. Biol.* 245:682–697.

Denisov, V. P., and B. Halle. 1995b. Hydrogen exchange and protein hydration: the deuteron spin relaxation dispersions of bovine pancreatic trypsin inhibitor and ubiquitin. *J. Mol. Biol.* 245:698–709.

Denisov, V. P., and B. Halle. 1995c. Direct observation of calcium-coordinated water in calbindin D9k by nuclear magnetic relaxation dispersion. *J. Am. Chem. Soc.* 117:8456–8465.

Denisov, V. P., and B. Halle. 1996. Protein hydration dynamics in aqueous solution. *Faraday Discuss.* 103:227–244.

Eidsness, M. K., A. E. Burden, K. A. Richie, D. M. Kurtz Jr., R. A. Scott, E. T. Smith, T. Ichiye, B. Beard, T. P. Min, and C. H. Kang. 1999. Modulation of the redox potential of the [Fe(SCys)(4)] site in rubredoxin by the orientation of a peptide dipole. *Biochemistry*. 38:14803–14809.

Elst, L. V., F. Maton, S. Laurent, F. Seghi, F. Chapelle, and R. N. Muller. 1997. A multinuclear MR study of Gd-EOB-DTPA: comprehensive preclinical characterization of an organ specific MRI contrast agent. *Magn. Res. Med.* 38:604–614.

Gonzalez, G., D. H. Powell, V. Tissieres, and A. E. Merbach. 1994. Water-exchange, electronic relaxation, and rotational dynamics of the MRI contrast agent [Gd(DTPA-BMA)(H2O)] in aqueous solution: a variable pressure, temperature, and magnetic field 17O NMR study. *J. Phys. Chem.* 98:53–59.

Guigliarelli, B., and P. Bertrand. 1999. Application of EPR spectroscopy to the structural and functional study of iron-sulfur proteins. *In* Adv. Inorg. Chem. A. G. Sykes and, R., Cammack, editors. Academic Press, San Diego. 421.

Halle, B., V. P. Denisov, and K. Venu. 1999. Multinuclear relaxation dispersion studies of protein hydration. *Biological Magnetic Resonance*. 17:419–483.

Hardcastle, K. I., M. Botta, M. Fasano, and G. Digilio. 2000. Evidence for a second coordination sphere water molecule in the hydration structure of YbDTPA. Insights for a reassessment of the relaxivity data of GdDTPA. *Eur. J. Inorg. Chem.* 971–977.

Hwang, L. P., and J. H. Freed. 1975. Dynamic effects of pair correlation functions on spin relaxation by transitional diffusion in liquids. *J. Chem. Phys.* 63:4017–4025.

Koenig, S. H., and R. D. Brown 3rd. 1990. Field-cycling relaxometry of protein solutions and tissue: implications for MRI. *Progr. NMR Spectrosc.* 22:487–567.

Koenig, S. H., R. D. Brown 3rd, and T. R. Lindstrom. 1981. Interactions of solvent with the heme region of methemoglobin and fluoromethemoglobin. *Biophys. J.* 34:397–408.

Kroes, S. J., J. Salgado, G. Parigi, C. Luchinat, and G. W. Canters. 1996. Electron relaxation and solvent accessibility of the metal site in wild-type and mutated azurins as determined from nuclear magnetic relaxation dispersion experiments. *J. Biol. Inorg. Chem.* 1:551–559.

Meyer, J., J. Gagnon, J. Gaillard, M. Lutz, C. Achim, E. Munck, Y. Petillot, C. M. Colangelo, and R. A. Scott. 1997. Assembly of a [2Fe−2S]2+ cluster in a molecular variant of Clostridium pasteurianum rubredoxin. *Biochemistry*. 36:13374–13380.

Min, T., C. E. Ergenekan, M. K. Eidsness, T. Ichiye, and C. Kang. 2001. Leucine 41 is a gate for water entry in the reduction of Clostridium pasteurianum rubredoxin. *Protein Sci.* 10:613–621.

Otting, G. 1997. NMR studies of water bound to biological molecules. *J. Am. Chem. Soc.* 31:259–285.

Otting, G., and E. Liepinsh. 1995. Protein hydration viewed by high-resolution NMR spectroscopy: implications for magnetic resonance image contrast. *Acc. Chem. Res.* 28:171–177.

Qian, Y. Q., G. Otting, and K. Wüthrich. 1993. NMR detection of hydration water in the intermolecular interface of a protein-DNA complex. *J. Am. Chem. Soc.* 115:1189–1190.

Sieker, L. C., R. E. Stenkamp, and J. LeGall. 1994. Rubredoxin in crystalline state. *Methods Enzymol.* 243:203–216.

Venu, K., V. P. Denisov, and B. Halle. 1997. Water 1H magnetic relaxation dispersion in protein solutions. A quantitative assessment of internal hydration, proton exchange, and cross-relaxation. *J. Am. Chem. Soc.* 119:3122–3134.

Wüthrich, K., G. Otting, and E. Liepinsh. 1992. Protein hydration in aqueous solution. *Faraday Discuss.* 93:35–45.

Xia, B., W. M. Westler, H. Cheng, J. Meyer, J. M. Moulis, and J. L. Markley. 1995. Detection and classification of hyperfine-shifted 1H, 2H, and 15N resonances from the four cysteines that ligate iron in oxidized and reduced Clostridium pasteurianum rubredoxin. *J. Am. Chem. Soc.* 117:5347–5350.

Xiao, Z., A. R. Gardner, M. Cross, E. M. Maes, R. S. Czernuszawicz, M. Sola, and A. G. Wedd. 2001. Redox thermodynamics of mutant forms of the rubredoxin from Clostridium pasteurianum: identification of a stable Fe(III)(S-Cys)3(OH) centre in the C6S mutant. *J. Biol. Inorg. Chem.* 6:638–649.

Xiao, Z., M. J. Lavery, M. Ayhan, S. D. B. Scrofani, M. C. J. Wilce, J. M. Guss, P. A. Tregloan, G. N. George, and A. G. Wedd. 1998. The rubredoxin from Clostridium pasteurianum: mutation of the iron cysteinyl ligands to serine. crystal and molecular structures of oxidized and dithionite-treated forms of the Cys42Ser mutant. *J. Am. Chem. Soc.* 120:4135–4150.

Zewert, T. E., H. B. Gray, and I. Bertini. 1994. Environment of the heme in myoglobins. NMRD and EPR spectroscopy of Val68X (X = Asn, Asp, and Glu). Mutants of human myoglobin. *J. Am. Chem. Soc.* 116:1169–1173.